

Exciton equilibration in the light-harvesting complex of Photosystem II of higher plants

Gerhard Kehrberg ^{a,*}, Joachim Voigt ^b, Thorsten Schrötter ^b, Gernot Renger ^c

^a *Institut für Optik und Spektroskopie Fachbereich Physik, Humboldt Universität zu Berlin, Berlin, Germany*

^b *Fachhochschule Brandenburg, Magdeburger Straße 53, 14770 Brandenburg, Germany*

^c *Max-Vollmer-Institut für Biophysikalische und Physikalische Chemie, Technische Universität Berlin, Berlin, Germany*

Received 30 November 1994; revised 11 April 1995; accepted 13 April 1995

Abstract

The exciton equilibration in the major chlorophyll *a/b* light-harvesting complex from spinach thylakoid membranes was analysed by non-linear transmission spectroscopy and pump-probe spectroscopy under quasi-stationary conditions at room temperature. Investigations of the non-linear transmission in the Q_y transitions of Chl *a/b* absorption indicate that excited state absorption dominates in the wavelength regions between 620 nm and 650 nm and between 685 nm and 690 nm, whereas bleaching and stimulated emission is predominant from 650 nm to 685 nm. The pump-probe transmission spectra suggest that in isolated light-harvesting complexes of Photosystem II (LHC II) the excitons are thermally equilibrated over all spectral chlorophyll forms nearly independent of the excitation wavelength. An analogous phenomenon is not observed in Photosystem II (PS II) membrane fragments. Regardless of differences between isolated LHC II and PS II membrane fragments in both samples, the maximum of the exciton density is located at around 680 nm independent of excitation intensity and wavelength. The maximum of exciton distribution in the Chl *b* absorption region is located at the absorption maximum of Chl *b* at 650 nm. The room-temperature exciton equilibration in the wavelength region of Chl *a* absorption can be described by a Boltzmann distribution. On the other hand, an inclusion of the Chl *b* excitons in the same distribution can be achieved only under the assumption of a strongly increased oscillator strength of Chl *b* states.

Keywords: Light-harvesting complex; Exciton migration; Pump and probe beam spectroscopy; Non-linear transmission

1. Introduction

The transformation of light into electrochemical free energy comprises the formation of electronically excited states and their transfer to the photochemically active pigment where the separation into an electron-hole pair takes place which has to be stabilised by subsequent electron transfer reactions in the dark. In order to assure an efficient trapping of light and to permit optimal adaptation to different illumination conditions, photosynthetic organism have developed suitable antenna systems. These systems consist of pigment-protein complexes which efficiently funnel the electronic excitation energy into the

reaction centre, thereby enhancing the apparent optical cross-section of the photoactive pigment by about two orders of magnitude. The excitation energy is equilibrated in few picoseconds among the chemically or environment induced spectroscopically different pigments within antenna-pigment-protein complex [1,2].

Different types of antenna have been developed during the evolution from photosynthetic bacteria up to the level of higher plants. In the latter species the antenna are formed by a complex array of different integral Chl *a* proteins containing mainly Chl *b* and carotenoids as accessory pigments (for recent studies see Ref. [3–5]). Pigment content per polypeptide (3–20 pigments) and abundance of individual pigment proteins as constituents of the antenna depend on the type of subunit [6]. The dominant part of the system II antenna is the light-harvesting complex II (LHC II) which comprises more than half of the total chlorophyll content. Compared with other subunits the LHC II is enriched with Chl *b*. LHC II was shown to form trimers of monomeric subunits each containing at least 12 chloro-

Abbreviations: Chl, chlorophyll; FWHM, full width at half maximum; LHC II, light-harvesting pigment protein complex of Photosystem II; P680, primary electron donor of reaction centre II; PS II, Photosystem II; CP, chlorophyll protein complex

* Corresponding author. Fax: +49 3381 26999.

phylls [7]. It is connected with the reaction centre complex of PS II via other pigment proteins of lower chlorophyll content (referred to as CP 24, CP 26 and CP 29) presumably acting as linkers (for a recent review see Ref. [6]). A PS II complex functionally competent in 'stable' charge separation ($P680^+$ Pheo Q_A^-) not only contains the polypeptides D1 and D2 as the matrix of the redox groups participating in this reaction, but is also intimately coupled with two Chl *a* proteins (CP 47 and CP 43) which are assumed to act as core antenna (for recent review see Ref. [8]).

The mode of structural organisation firstly permits an adaptation of the antenna size to prevailing illumination conditions (e.g., 'light' and 'shade' plants). In addition, the lateral distribution of pigment-protein complexes within the thylakoid membrane and its modification via protein phosphorylation regulates the distribution of excitation energy between Photosystem I and II (for recent review see Ref. [9] and references cited therein). A thorough mechanistic understanding of the excitation energy transfer processes requires detailed information on the structure of the pigment proteins, especially the distance and mutual orientation of the pigment molecules and their mode of embedding into the protein matrix. Although significant progress has been achieved due to both the improvement of the isolation procedures of these proteins and the advancement of laser spectroscopy with high resolution in the time and frequency domain (for reviews see [10–12]), some relevant mechanistic questions are still not satisfactorily answered. Among them, the fundamental problem of coherent contributions to the overall excitation energy transfer is a matter of debate [13,14]. The mode of this process strongly depends on the strength of pigment interaction which can give rise to exciton coupling. Recent results on the antenna protein monomer of *P. aestuarii* [15] and of the PS II antenna complexes [16] suggest that the pattern of excitation energy transfer within the protein monomers is complex. In both antenna complexes, spectral Chl forms were found that originate from strongly coupled pigments with highly delocalised excitons and those that can be ascribed to 'isolated' (in terms of exciton coupling pigments with more 'localised') excited states. The physiological function of this mixture of different excitation states is not clear. The excitonic coupling of pigments depends on their distance and mutual orientation. At present, detailed structural information on chlorophyll protein complexes of the PS II antenna is available only for LHC II. Electron crystallography data of two-dimensional crystals at 0.34 nm resolution reveal that the porphyrin rings of 12 (13?) chlorophyll molecules in each monomeric subunit are arranged in two layers with pigment-pigment distances of 0.9–1.4 nm [7]. This indicates that the electronic coupling between chlorophyll molecules can attain a considerable strength. Therefore, LHC II preparations provide a suitable material for the study of their electronic levels and the distribution of excitation energy.

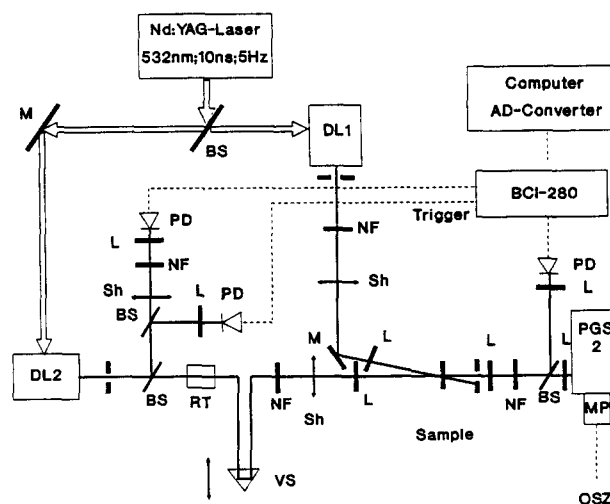


Fig. 1. Experimental set-up (BS beamsplitter, M mirror, L lens, VS optical delay line, Sh shutter, MP photomultiplier; for more details see text).

In the present study comparative measurements were performed of the non-linear optical properties of isolated LHC II complexes and PS II membrane fragments. The results obtained are discussed within the framework of excitonic coupling between pigments and the distribution of excitation energy among the different electronic levels of LHC II. Marked differences in the properties were found between LHC II and PS II membrane fragments. These findings are analysed and discussed.

2. Materials and methods

PS II membrane fragments were isolated from spinach by the method of Berthold et al. [18] with slight modifications as described by Irrgang et al. [19]. LHC II proteins have been separated after β -DM solubilisation (detergent/Chl ratio 10:1 (w/w)) of salt-washed (NaCl and $CaCl_2$) PS II membrane fragments by sucrose density gradient centrifugation in the presence of 0.05% β -DM.

A comparison of 77 K fluorescence spectra (not shown) with data reported in the literature [20] reveal that the isolated LHC II complexes used in the study are in the form of non-aggregated trimers.

The non-linear one- and two-beam absorptions were measured at a temperature of about 5°C with the experimental set-up shown in Fig. 1. The nanosecond pulses of the pump and probe beam, variable in wavelength, were generated by using two dye laser grating resonators (DL) with grazing incidence (FWHM 10 ns) pumped by the second harmonic of the output from a Nd^{3+} :YAG-laser (model 501-D.NS 710, B.M.Industries). Both dye lasers had spectral half width of about 0.01 nm and an energy of 40 μ J, giving a maximum density of about $1 \cdot 10^{19}$ pho-

tons per cm^2 per pulse when focused on a spot of about 0.04 mm in diameter. This corresponds to about 150 photons per Chl and pulse under our experimental conditions. The intensity ratio of the dye lasers was about 3000:1 between the peak and the background at a wavelength difference of ± 3 nm. The repetition rate of pulses was 5 Hz. The polarisation ratio was 10:1. The probe beam was focused at an angle of 5° into a spot of 0.04 mm in diameter inside the spot of the pump beam. Under these conditions the probe beam had about $1 \cdot 10^{15}$ photons per cm^2 per pulse. This is sufficient to induce a detectable non-linear fluorescence (not shown here). The coincidence of both beams in time and area was ensured with great care by control experiments where both beams were focused on a pinhole and adjusted by using a microscope. The pump beam can be simply separated from the probe beam by a diaphragm if the sample scattering is sufficiently small. In the case of samples with strong scattering (PS II membrane fragments) the pump beam was separated by a grating spectrometer (PGS2) with a linear dispersion of 0.36 nm/mm. All signals were detected by integrated silicon diode/amplifier-receivers (model 712A-2, Analog Module, INC.; PD) and amplified by boxcar integrators (model BCI 280, ZWG) at fixed gate position. Reference beams were obtained by splitting off a fraction of the probe and pump laser beam before the sample cuvette. In order to correct for power fluctuations in the probe and pump beam, the detected transmittance signal at each wavelength was normalised by using the digitised reference signals.

Calcite prism polarisers were used to clean up the vertical polarisation of the pump and probe beams. The polarisation plane of the probe beam was adjusted parallel to that of the pump beam (using a Soleil-Babinet compensator Carl Zeiss Jena; RT).

The relative transmission in two-colour experiments is calculated by the formula:

$$T_{\text{two}}^{\text{rel}} = (I_{\text{p+pr}} - I_{\text{p}}) / I_{\text{pr}} \quad (1)$$

where $I_{\text{p+pr}}$ and I_{pr} are the intensities of the probe beam transmitted through the sample, in the presence and absence of the pump beam, respectively. I_{p} is the intensity of the amplified spontaneous emission of the pump dye laser at the wavelength of the probe beam.

In another type of experiment the non-linear absorption was measured as a function of the excitation density. In this case, only one laser beam was used and the intensity of the laser was varied over 7 orders of magnitude by computer-controlled neutral density filters (NF). The lowest value I was chosen to be in the linear region of transmission. The relative transmission in one-colour experiment was calculated by the expression:

$$T_{\text{one}}^{\text{rel}} = T / T_{I \rightarrow 0} \quad (2)$$

where $T_{I \rightarrow 0}$ and T are the transmittance at the range of linear and non-linear transmission, respectively. In princi-

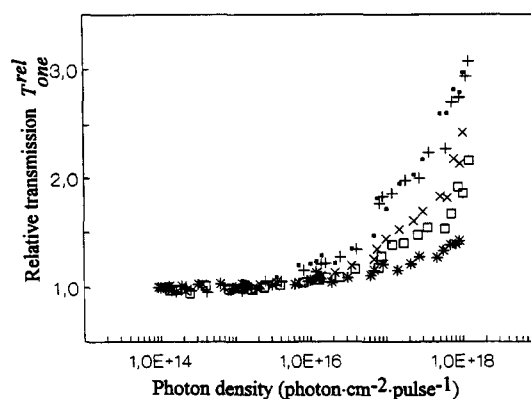


Fig. 2. Relative transmission $T_{\text{one}}^{\text{rel}}$ of LHC II as a function of photon density at different wavelengths (*, 665 nm; ×, 670 nm; ■, 675 nm; +, 680 nm; □, 685 nm).

ple, single-beam non-linear absorption experiments are pump-probe experiments with variable pump beam intensity and *same* wavelengths of pump and probe beam.

3. Results

In a pump-probe experiment, the following effects can contribute to a transmission change of the probe beam at a particular wavelength:

1. absorption due to the population of excited states,
2. stimulated emission and
3. bleaching due to ground state depopulation.

The extent of these contributions depends on the system of the electronic levels and the excitation intensity. The same physical processes are responsible for transmission changes measured in single-beam experiments.

3.1. One-colour measurements

One-colour measurements were performed as a function of photon density at five different wavelengths (665, 670, 675, 680 and 685 nm) in suspensions of LHC II and PS II membrane fragments. The results obtained are depicted in Fig. 2 (LHC II) and Fig. 3 (PS II membrane fragments). Both sample types exhibited a strong enhancement of the relative transmission $T_{\text{one}}^{\text{rel}}(I)$ with increasing photon densities, I . Interestingly, in the wavelength region of 665–685 nm neither a decrease nor a saturation of the relative transmission was observed up to the highest photon densities available. This indicates that stimulated emission and bleaching due to ground-state depopulation are the dominating factors. Their relative contribution to the overall effect cannot be separated. The observed phenomena are more precisely described as non-linear transmission rather than as non-linear absorption, because we cannot rule out small high-intensity-induced reflection and scattering changes in our experiments.

Although in most molecular systems stimulated emission at the laser wavelength itself is assumed to be not significant because of the rapid conversion between vibrationally coupled sublevels [21], this is not necessarily the case in our sample material.

A closer inspection of Fig. 2 and Fig. 3 reveals differences between both sample types with respect to the excitation wavelength dependence of the derivations from linearity ('onset' of non-linearity). Therefore, this 'onset' was used as a rough phenomenological parameter to describe the differences between both sample types. In LHC II the relative transmission $T_{\text{one}}^{\text{rel}}(I)$ arises above threshold photon densities between $2 \cdot 10^{16}$ and $6 \cdot 10^{16}$ photons per cm^2 per pulse with a rather weak dependence on the excitation wavelength. On the other hand in PS II membrane fragments the 'onset' of the relative transmission $T_{\text{one}}^{\text{rel}}(I)$ exhibits a marked wavelength dependence. It decreases by about two orders of magnitude toward smaller photon densities of the pump pulse if the wavelength increase from 665 to 680 nm (data not shown).

The results of Fig. 2 and Fig. 3 markedly differ from our previous measurements of the relative transmission at 620 nm and 647 nm, where a decrease is followed by an increase with increasing photon density [22]. In order to investigate the exact wavelength region where a transmission decrease (excited state absorption) might occur, measurements were performed as a function of the photon density in 2 nm steps in narrow wavelength regions around 650 nm and 686 nm, respectively. Fig. 4A–C shows the relative transmission at 647 nm, 649 nm and 651 nm, respectively, in LHC II. Even if one takes into account the experimental scatter of the data points, the results indicate that at 647 nm and 649 nm the transmission exhibits a small, but discernible decrease followed by a pronounced increase with rising photon densities of the pulse. These findings are in line with the general feature of our former studies [17,22,23]. As an extension of these measurements to the red edge, Fig. 5A,B shows the relative transmission effects in LHC II at 686 nm and 690 nm, respectively. At

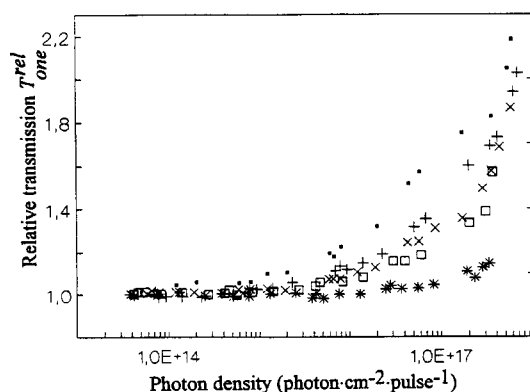


Fig. 3. Relative transmission $T_{\text{one}}^{\text{rel}}$ of PS II membrane fragments as a function of photon density at different wavelengths (*, 665 nm; x, 670 nm; ■, 675 nm; +, 680 nm; □, 685 nm).

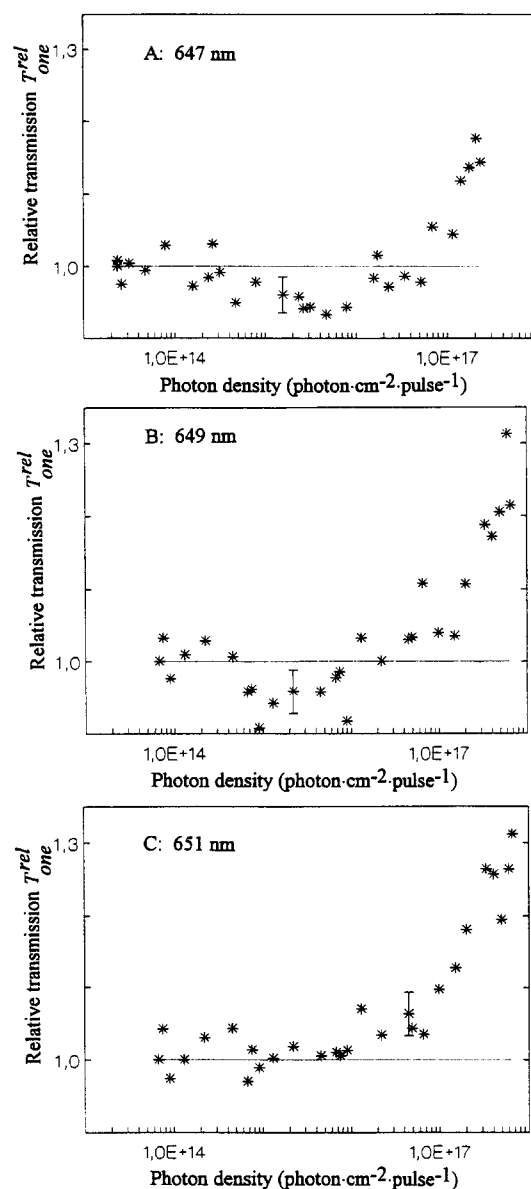


Fig. 4. Relative transmission $T_{\text{one}}^{\text{rel}}$ of LHC II as a function of photon density at different wavelengths (A: 647 nm; B: 649 nm; C: 651 nm).

both wavelength a dip of the transmission can be resolved within the rising part of the transmission at a photon density of about $8 \cdot 10^{17}$ photons per cm^2 per pulse. As this phenomenon is comparatively small, several experiments have been performed to show that this effect is real and reproducible. This feature contrasts with the relative transmission properties in the wavelength region between 650 nm and 685 nm, where no decrease could be observed at any photon density within the limits of our resolution of the measurements (compare Fig. 2 and Fig. 5A,B).

3.2. Two-colour measurements

For further analysis of exciton distribution two-colour experiments were performed. Fig. 6 shows the spectra of

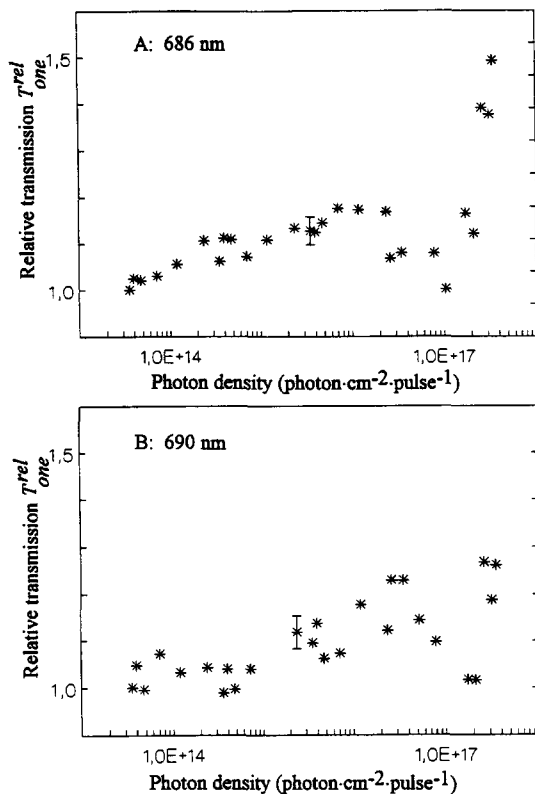


Fig. 5. Relative transmission T_{one}^{rel} of LHC II as a function of photon density at 686 nm (A) and 690 nm (B).

the relative probe beam transmission $T_{two}^{rel}(\lambda_{pr})$ induced in isolated LHC II preparations by a pump beam of constant photon density at three different wavelengths of 650, 660 and 680 nm, respectively. The probe beam transmission were measured in 2 nm steps. The use of a spectral continuum probe beam is impracticable, because the integral intensity of this beam would be too high for the region of linear absorption in molecular systems with highly efficient energy transfer. The photon densities used were $5.6 \cdot 10^{18}$ and $1 \cdot 10^{15}$ photons per cm^2 and per pulse in

the pump and probe beam, respectively. A striking feature of the spectra of $T_{two}^{rel}(\lambda_{pr})$ presented in Fig. 6 is the presence of two peaks at around $\lambda_{pr} = 650$ nm and $\lambda_{pr} = 680$ nm. It is important to note that only a weak dependence of the spectra of $T_{two}^{rel}(\lambda_{pr})$ exists on the pump pulse wavelength. Virtually, the same spectra are obtained at pump beam wavelength of 670 and 673 nm (not shown). The height and the peak position of $T_{two}^{rel}(\lambda_{pr} = 680$ nm) are nearly independent of the different used pump pulse wavelengths. In the wavelength region where Chl *b* significantly contributes to the absorption, i.e., between 640 and 660 nm, the differences appear to be more pronounced. In this spectral region the extent of $T_{two}^{rel}(\lambda_{pr})$ increases at shorter wavelength of the pump pulse (at $\lambda_p = 650$ nm the effect is about 30% higher than at $\lambda_p = 680$ nm, whereas in the long wavelength region the effect is of opposite direction, i.e., slightly smaller at $\lambda_p = 650$ nm compared with $\lambda_p = 680$ nm). Similar spectra were found by Lepold et al. on chloroplasts [24]. An additional feature is a small shoulder arising at 665 nm if the pump beam wavelength is at 660 nm.

A comparison of the spectra of $T_{two}^{rel}(\lambda_{pr})$ with the ground state absorption of LHC II shows that in the range of Chl *b* absorption both spectra are characterised by similar peak positions while in the case of Chl *a* absorption the peak of T_{two}^{rel} is shifted to the red by about 5 nm. Fig. 7 shows the corresponding spectra of $T_{two}^{rel}(\lambda_{pr})$ of PS II membrane fragments in the same probe beam wavelength region (640 to 690 nm). An inspection of the spectra readily shows that the striking red shift of the peak position of T_{two}^{rel} by about 5 nm compared with the Chl *a* absorption band is also observed in PS II membrane fragments (Fig. 7). However, in contrast to the LHC II complex, the spectra are now strongly dependent on the pump pulse wavelength. Furthermore, the spectra of $T_{two}^{rel}(\lambda_{pr})$ in Fig. 7 exhibit much smaller contributions in the 650 nm region (compared with the dominating 680 nm band) due to the higher Chl *a/b* ratio in PS II membrane

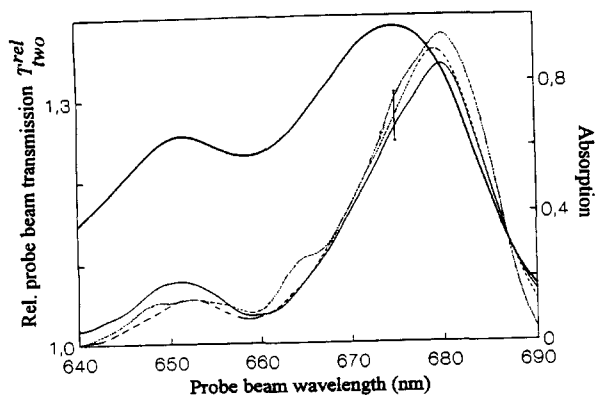


Fig. 6. Relative probe beam transmission T_{two}^{rel} of LHC II as a function of the probe beam wavelength at different pump beam wavelengths (—, 650 nm; ···, 660 nm; ---, 680 nm) additional to the absorption spectrum (—). Excitation intensity: $5.6 \cdot 10^{18}$ photons $\cdot \text{cm}^{-2} \cdot \text{pulse}^{-1}$.

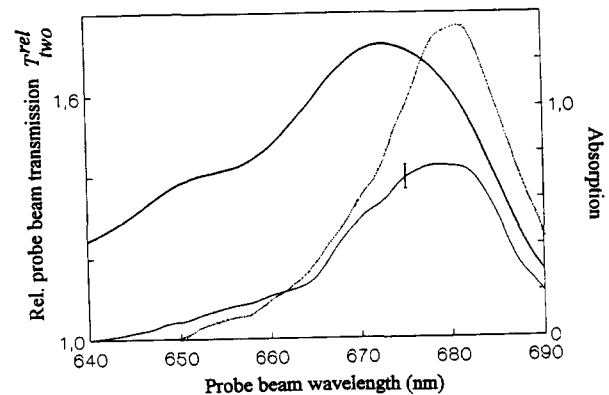


Fig. 7. Relative probe beam transmission T_{two}^{rel} of PS II membrane fragments as a function of the probe beam wavelength at different pump beam wavelengths (—, 650 nm; ---, 680 nm) and the absorption spectrum (—). Excitation intensity: $5.6 \cdot 10^{18}$ photons $\cdot \text{cm}^{-2} \cdot \text{pulse}^{-1}$.

fragments. The results of Fig. 6 and Fig. 7 reveal that the spectra of $T_{\text{two}}^{\text{rel}}(\lambda_{\text{pr}})$ exhibit a characteristic peak at about $\lambda_{\text{pr}} = 680$ nm independent of the pump pulse wavelength. In these experiments the photon density of the pump pulse was kept constant. Now it remains to be shown that this effect is not simply due to a shift by the high electric field strength of the pump pulse. Therefore, the spectra of the relative probe beam transmission were measured in LHC II suspensions excited with pump pulses of four different photon densities ($1.2 \cdot 10^{19}$, $7.4 \cdot 10^{18}$, $1.4 \cdot 10^{18}$ and $1.4 \cdot 10^{17}$ photons per cm^2 per pulse) and a wavelength of 650 nm. The results obtained are summarised in Fig. 8. It is obvious that the positions of the maxima at $\lambda_{\text{pr}} = 650$ nm and $\lambda_{\text{pr}} = 680$ nm in the spectra of $T_{\text{two}}^{\text{rel}}(\lambda_{\text{pr}})$ are virtually independent of the photon flux density. From this data, the position of the 680 nm peak in the spectra of $T_{\text{two}}^{\text{rel}}(\lambda_{\text{pr}})$ is inferred not to be caused by an electric-field-induced shift of the red Chl *a* absorption band.

In the inset of Fig. 8, a double logarithmic plot is shown of the logarithm of the relative probe beam transmission at $\lambda_{\text{pr}} = 650$ nm and $\lambda_{\text{pr}} = 670$ nm, respectively, as a function of the photon density of the pump beam at a wavelength of 650 nm. The slope in the region of the Chl *b* band is about 1, while that in the region of dominating Chl *a* absorption is only about 0.5. This finding could be explained by the assumption that exciton annihilation of Chl *b* excitons is considerably smaller than that of Chl *a* excitons.

The decrease of $T_{\text{two}}^{\text{rel}}$ at probe beam wavelengths longer than 685 nm at higher pump beam intensities under the value of $T_{\text{two}}^{\text{rel}}$ at the lowest used intensity is caused by dominating excited state absorption. This feature corresponds with those of the 'one-colour' measurements in the same wavelength region (compare Fig. 5A,B with Fig. 8).

For the experimental set-up used in this study, another

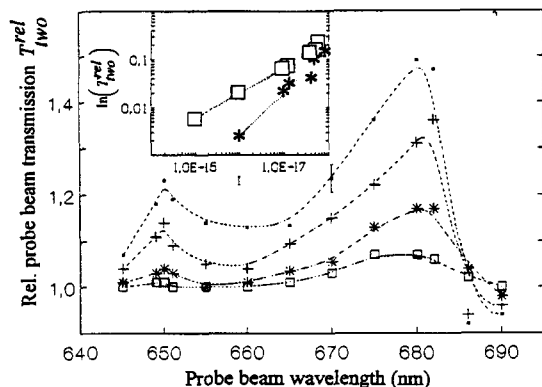


Fig. 8. Relative probe beam transmission $T_{\text{two}}^{\text{rel}}$ of LHC II as a function of wavelength at different pump beam photon densities (\blacksquare , $1.2 \cdot 10^{19}$; $+$, $7.4 \cdot 10^{18}$; $*$, $1.4 \cdot 10^{18}$; \square , $1.4 \cdot 10^{17}$ photons $\text{cm}^{-2} \cdot \text{pulse}^{-1}$); pump beam wavelength 650 nm. Inset: double logarithmic plot of the logarithm of relative probe beam transmission $\ln(T_{\text{two}}^{\text{rel}})$ as a function of the pump beam photon density at different probe beam wavelengths ($*$, 650 nm, slope = 0.95; \square , 670 nm, slope = 0.52).

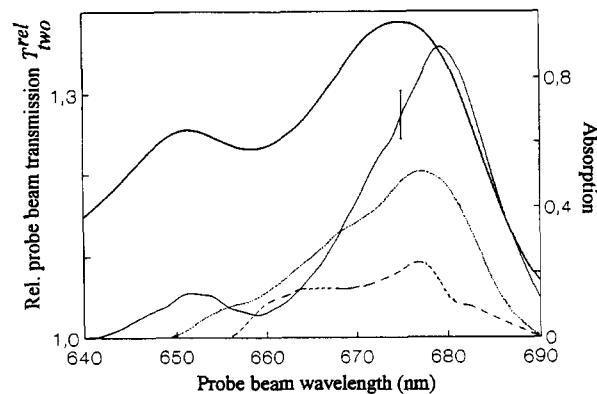


Fig. 9. Relative probe beam transmission $T_{\text{two}}^{\text{rel}}$ of LHC II as a function of the probe beam wavelength at different delay times between pump and probe beam ($-$, 0 ns; \cdots , 5 ns; $--$, 13 ns); absorption spectrum ($- \cdot -$); pump beam wavelength, 680 nm.

effect has to be taken into consideration. At a pulse duration of 10 ns triplet states can be populated to a considerable extent [25]. In order to analyse the contribution of ground state depletion due to population of triplet states as well as transitions between triplet states to the spectra of $T_{\text{two}}^{\text{rel}}(\lambda_{\text{pr}})$, the relative probe beam transmission was measured in LHC II at different delay times between pump and probe pulse. Pump beam wavelength $\lambda_{\text{p}} = 680$ nm and pump beam intensity of $5.6 \cdot 10^{18}$ photons $\cdot \text{cm}^{-2} \cdot \text{pulse}^{-1}$ were fixed. The results shown in Fig. 9 reveal that the maximum of $T_{\text{two}}^{\text{rel}}(\lambda_{\text{pr}} = 680 \text{ nm})$ at delay time $\Delta t = 0$ is shifted towards shorter wavelengths at increasing delay times and the feature of the spectrum of $T_{\text{two}}^{\text{rel}}(\lambda_{\text{pr}})$ is drastically changed. The maximum of $T_{\text{two}}^{\text{rel}}$ at $\lambda_{\text{pr}} = 650$ nm totally disappears. At delay time $\Delta t = 13$ ns it is reasonable to assume that singlet excitons generated by the pump pulse in the LHC II sample decayed to more than 95% and the spectrum of $T_{\text{two}}^{\text{rel}}(\lambda_{\text{pr}})$ is significantly affected by triplet excitons. This spectrum is therefore a qualitative measure of the 'triplet state contamination' in the spectrum of $T_{\text{two}}^{\text{rel}}(\lambda_{\text{pr}})$ at $\Delta t = 0$. A comparison of both spectra reveals that in terms of the general shape the contribution of triplet excitons to the spectrum at $\Delta t = 0$ can be considered to be comparatively small.

For the following discussion of the results it appears reasonable to assume that in the case of PS II membrane fragments a pulse duration of 10 ns leads to a quasi-steady state excited singlets. The absence of an asymmetric temporal shaping of the laser pulse transmitted through the sample (data not shown) confirms that the non-linear transmission measured by using pulses of about 10 ns duration is really a quasi-steady-state process. In the case of LHC II complexes the situation is more complex. The lifetime of LHC II preparations used in this study is dominated (about 90% of the total decay) by a 4.3 ns lifetime [26]. This value is of the order of the pulse duration and therefore the assumption of quasi-steady state

conditions can be only considered as a very rough approximation for LHC II. However, in terms of exciton equilibration among the electronic levels of the pigments within the LHC II the assumption of quasi-steady state conditions is still justified because the excitation energy transfer processes and relaxation take place in the picosecond and even subpicosecond time domain [27],[28].

4. Discussion

Based on the measurements of pump pulse induced non-linear transmission phenomena presented in this study and taking into account data from the literature an attempt will be made to analyze qualitatively properties and interactions of lowest excited singlet states of Chl *a* and Chl *b* in the antenna system of PS II. The 'one-colour' and 'two-colour' pump-probe experiments in the frequency domain performed under quasistationary conditions of excited singlet states (FWHM of pulses 10 ns) in suspensions of isolated LHC II and PS II membrane fragments led to several interesting results and implications. Before discussing these results it seems worth adding some remarks with respect to the comparability between the non-linear experiments presented in this study and conventional (low-power) experiments.

1. In both types of experiment the pump beam intensity must be high enough to reach a population of the first excited state. Therefore both types are non-linear optical experiments in the sense that the absorption coefficient α will be a function of the pump pulse intensity.
2. The difference between the conventional experiments and the experiments described in this paper is the much higher pump pulse intensity in the latter. Under the latter conditions, excited-state absorption and exciton-exciton-annihilation of the chlorophyll excitations have to be taken into account as essential processes, whereas in conventional pump-probe experiments these phenomena are of minor relevance.

4.1. Non-linear transmission effects in 'one-colour' experiments

The results presented in Figs. 2–5 and our previous data [22,23] reveal that the non-linear optical properties of the PS II antenna exhibit characteristic spectral features with marked differences in their dependence on the excitation intensity:

1. in the wavelength region of significant Chl *b* absorption (620–650 nm) the laser pulse causes a small decrease of transmission at photon densities of the order of 10^{16} photons per cm^2 and per pulse. At higher photon densities a transmission increase is observed,
2. in the wavelength region of 650–685 nm no decrease of transmission is observed at any photon density applied in this study.

3. at wavelengths longer than 685 nm the increase is superimposed by a dip at photon densities of about 10^{18} photons per cm^2 and per pulse.

Qualitatively similar features were observed in isolated LHC II preparations by using a pump-probe pulse technique with high time resolution [28]. It has been found that the transmission decreases in the range of 645–655 nm at delay times between pump and probe pulse of shorter than 5 ps, while under the same conditions the transmission increases in the wavelength region of 655–675 nm. However, these data cannot be directly compared with the present results because of the quite different experimental conditions (transient effects in the short time domain versus quasistationarity in 10 ns pulses) and the lack of information on the non-linear transmission as a function of the photon density in the short-pulse experiments of Ref. [28].

The striking phenomenon of different dependencies on the excitation intensity of the non-linear absorption/stimulated emission in the short and long wavelength region versus that in the range of 655–680 nm (decrease and subsequent increase of the transmission versus exclusive increase with increasing photon densities, respectively) is not a peculiar property of the LHC II complex because similar features were observed in the antenna system of the anoxygenic green sulfur bacterium *Chloroflexus aurantiacus* [29]. In this case, the pump-probe-pulse experiments were also performed at high time resolution so that transient nonequilibrium states are monitored. On the other hand, the experiments of present study were performed under conditions where the non-linear transmission is mainly determined by electronic states which are thermally distributed over the whole pigment ensemble.

A quantitative analyses of the non-linear optical properties of the electronic structure of the interacting pigments are beyond the scope of this study (a more thorough calculation will be presented in a forthcoming paper). Therefore, the results will be discussed in a more qualitative way.

The phenomenon of a non-linear transmission decrease induced by a strong laser pulse can be simply explained by excited state absorption. At high photon densities excited states become increasingly populated.

Simultaneously the stimulated emission (σ_{10}) also increases. In order to observe a net transmission decrease the condition $\sigma_{12} > \sigma_{01} + \sigma_{10}$ has to be satisfied, where σ_{12} and σ_{01} represent the optical cross-sections for the transitions $S_1 \rightarrow S_n$ ($n \geq 2$) and $S_0 \rightarrow S_1$, respectively [17]. This simple relation describes the properties of a system of isolated pigment molecules with three or more electronic levels. In the case of chlorophyll in solution (pyridine) the value of σ_{12} exceeds that of $\sigma_{01} + \sigma_{10}$ for $\lambda < 650$ nm and $\lambda > 680$ nm [30]. Therefore, under suitable conditions a laser-pulse-induced transmission decrease can be observed in Chl solutions. In pigment-protein complexes, however, additional effects have to be taken into account,

depending on the strength of the electronic interaction between the pigment molecules. This effect can give rise to excitonic splitting, i.e., the electronic levels of the antenna complex cannot be satisfactorily described by the levels and oscillator strengths of the individual pigments in the case of significant excitonic coupling. Therefore, at high photon densities a complex pattern of interacting excitons gives rise to the overall non-linear transmission. Therefore we suggest that, in pigment protein complexes, the transition $S_1 \rightarrow S_2$ means a 1-exciton \rightarrow 2-exciton transition and σ_{12} is the optical cross-section for this transition. This type of model has been applied in order to interpret the non-linear transmission as function of the photon density of LHC II preparations and PS II membrane fragments in the range of 620–650 nm [17,22,30,31].

Another effect that cannot be explained with the above-mentioned assumption is the dip of the transmission decrease superimposed on the rising part observed in the long wavelength region (686 nm and 690 nm, see Fig. 6). This finding indicates that more a complex pattern of the electronic levels arises including a mixture of excitonic and nonexcitonic interactions between Chl-molecules [5] interfered by on-diagonal and off-diagonal disorder analogously to the BChl *a* protein trimer in the antenna of *Prosthecochloris aestuarii* [15].

An interesting feature emerges from a comparison between isolated LHC II preparations and PS II membrane fragments in terms of their wavelength dependence of the photon densities required for the 'onset' of the relative transmission $T_{\text{one}}^{\text{rel}}(I)$. The value of this threshold photon density was nearly independent of the wavelength in isolated LHC II, while a remarkable variation over two orders of magnitude is observed in PS II membrane fragments (see Fig. 4). The latter phenomenon seems to reflect an increasing population probability of excited states at long wavelength absorbing fragments. These species are probably located in the Chl *a* containing protein complexes CP 47 and CP 43. This idea is also supported by the two-colour experiments.

4.2. Non-linear transmission effects in 'two-colour' experiments

The spectra of the probe beam transmission $T_{\text{two}}^{\text{rel}}(\lambda_{\text{pr}})$ presented in Figs. 6–8, permit a first attempt to determine the excited state distribution under quasi-steady state equilibration conditions in isolated LHC II complexes and PS II membrane fragments. The spectra of $T_{\text{two}}^{\text{rel}}(\lambda_{\text{pr}})$ (Fig. 6) reveal that under these conditions the distribution among the lowest excited singlet state levels ascribed to Chl *a* in LHC II are nearly independent of the pump pulse wavelength. A markedly different behaviour is observed in pump-probe experiments in the time domain of about 100 ps. In this case a non-Boltzmann distribution among the Chl *a* excited singlet states S_1 arises at pump wavelengths of 650 and 665 nm [27].

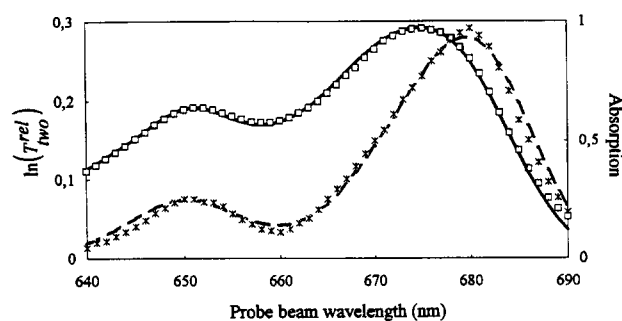


Fig. 10. Absorption spectrum (\square measured; — calculated) and spectrum of logarithm of relative probe beam transmission $\ln(T_{\text{two}}^{\text{rel}}(\lambda_{\text{pr}}))$ (* measured; — — calculated) of LHC II as a function of the probe beam wavelength; pump beam wavelength: 650 nm, pump beam intensity: $5.6 \cdot 10^{18}$ photons \cdot cm $^{-2}$ \cdot pulse $^{-1}$; conditions for calculations, see text.

In contrast to the behaviour of isolated LHC II complexes, the steady state distribution of lowest excited singlet states in PS II membrane fragments exhibits a rather strong dependence on the pump pulse wavelength (see Fig. 7). This finding could imply that a Boltzmann type equilibration cannot be achieved within PS II even under quasi-stationary conditions. A support of this idea is the conclusion (derived from a fluorescence study) that the energy transfer to the PS II reaction centre is a function of the excitation wavelength (with the longer wavelength being more efficient [32]).

In the following a semiquantitative analysis will be presented based on a simplified model. The spectrum of $T_{\text{two}}^{\text{rel}}(\lambda_{\text{pr}})$ is fitted (as shown in Fig. 10) by using the equation:

$$\ln(T_{\text{two}}^{\text{rel}}(\lambda_{\text{pr}})) = \sum_i \alpha_i(\lambda_{\text{pr}}) \cdot d \cdot f_i \cdot g_i \quad (3)$$

where α_i is the absorption coefficient, obtained by a deconvolution of the absorption spectrum into Gaussian bands (fitted absorption spectrum see Fig. 10). d is the optical path length, f_i the Boltzmann distribution function and g_i a fit parameter. The term $\sum_i \alpha_i(\lambda_{\text{pr}}) \cdot d \cdot f_i$ can be easily obtained from Eqn. 1. under the assumption of a two level energy scheme and Boltzmann distributed excited states. In correspondence with data from literature [5] the following band maxima are used: 640 nm ($g_i = 5$), 650 nm ($g_i = 11$), 657 nm ($g_i = 1$), 662 nm ($g_i = 1$), 669 nm ($g_i = 0.9$), 676 nm ($g_i = 1$) and 683 nm ($g_i = 1.5$). A good fit of the spectrum of $T_{\text{two}}^{\text{rel}}(\lambda_{\text{pr}})$ (Fig. 10) can be achieved with the g_i -values given in parentheses. In the Chl *a* absorption region the correction factor g_i is close to 1, in contrast to the Chl *b* absorption region, where a marked increase of g_i is required. However, the extend of g_i in the Chl *b* absorption region is unrealistically high. In our opinion, the correction factor describes the influence of additional optical transitions caused by the high pump intensity for instance excited state absorption or two particle excitations. A deviation of the distribution of excited states from a Boltzmann distribution seems improbable.

Apart from any model-dependent interpretation, however, another striking feature emerges from the results presented in this study, i.e., the maximum of excited state distribution among the Chl *a* molecules of isolated LHC II is virtually independent of the wavelength of the pump pulse. Furthermore, compared with the red maximum of the ground-state absorption at around 676 nm, the peak in the spectrum of $T_{\text{two}}^{\text{rel}}(\lambda_{\text{pr}})$ is shifted by about 5 nm towards longer wavelength (see Fig. 6). This finding suggests that the Chl *a* excitons relax into an energy level of slightly lower energy. Interestingly, the spectral maximum of the relative probe beam transmission corresponds with that of P680. Therefore, a rather high population of excited states is created in the antenna at the energy level coinciding with that of $^1\text{P680}^*$. Accordingly, this mode of energy distribution is in line with the concept of a rather shallow exciton trap in PS II [33].

In contrast to LHC II, however, the shape of the spectrum of $T_{\text{two}}^{\text{rel}}(\lambda_{\text{pr}})$ in PS II membrane fragments now strongly depends on the wavelength of the pump pulse. The enhanced excited state population at longer wavelengths of the pump pulse (see Fig. 7) is probably due to the presence of the core antenna (CP 43 and CP 47) in PS II membrane fragments. The LHC II preparations are absolutely free of CP43 and CP47 but contain some contamination of minor Chl-binding proteins of the distal antenna (CP29, CP26, CP24). That do not significantly affect the optical properties. A closer inspection shows that the larger optical cross-section of PS II membrane fragments (compared of the data with LHC II) cannot fully account for the markedly higher excited state population caused by long wavelength photons (670–680 nm). Therefore, further investigations are required to clarify this phenomenon.

In summary, the data of the present study show that under quasistationary conditions excited states become preferentially populated which are practically isoenergetic with P680. The details of the underlying mechanism and especially the marked deviations in the region of Chl *b* absorption remain to be clarified by further experimental and theoretical investigations.

5. Conclusions

The principal features of the one-colour and two-colour non-linear transmission experiments on LHC II trimers and on PS II membrane fragments may be summarised as follows:

1. The excitons are equilibrated in the antenna of PS II with a population maximum at 680 nm which is independent of the excitation wavelength. This large population probability of the excitons in that energetic position is very convenient for the trap-limited transfer process in the RC II promoting the conclusion that the primary donor of the RC II is a very shallow trap [33].
2. The relative probe beam transmission of the Chl *b* exciton states in LHC II complexes is much higher independent of the pump beam wavelength than expected by fitting the exciton equilibration with a room-temperature Boltzmann-distribution. That means the equilibration of excited singlet states (S_1) over the whole ranges of Chl *a/b* absorption in the red comprises a significant contribution of uphill energy transfer. Alternatively, this phenomenon could be also interpreted as indicating that the lowest-energy exciton states have significant admixtures of Chl *b* excitations.
3. In PS II membrane fragments the exciton distribution depends strongly on the excitation wavelength with a higher exciton population for longer wavelengths. This may reflect either the presence of the core antenna in PS II membrane fragments or another structural arrangement of the protein-chlorophylls. The higher efficiency of long-wavelength photons (670–680 nm) for the exciton population at 680 nm is much larger than expected to be by the higher absorption cross-section in this region as shown by the strong wavelength dependence of the non-linear transmission on PS II membrane fragments.
4. The one-colour intensity-dependent experiments $T_{\text{one}}^{\text{rel}}(I)$ provide different wavelength-dependences of the relation between ground state and excited state absorption. A simple description of the cross-section of the excited state and ground absorption to be caused by the well-known different absorption cross-sections of individual chlorophylls in the short and long-wavelength region is not possible, as shown in our previously paper [22,23]. Proceeding from this, we think that this non-linear absorption behaviour is governed by the physics of strong Chl–Chl interactions, at least within a monomeric protein.

Acknowledgements

We thank Drs. Elisabeth Haag and Klaus-Dieter Irrgang (Max-Volmer-Institut, Technische Universität Berlin) for providing the sample material used in this study. This work was financially supported by the Deutsche Forschungsgemeinschaft (Sonderforschungsbereich 312, TP A2 and TP A6).

References

- [1] Gillbro, T., Sundström, V., Sandström, A., Spangfort, M. and Andersson, B. (1985) FEBS Lett. 193, 267–270.
- [2] Van Grondelle, R., Dekker, J.P., Gillbro, T. and Sundström, T. (1994) Biochim. Biophys. Acta 1187, 1–65.
- [3] Thornber, J.P. (1986) in Photosynthesis III, Encyclopaedia of Plant Physiology (Staehelin, L.A. and Arntzen, J.P., eds.), Vol. 19, pp. 98–142, Springer, Berlin.

- [4] Bassi, R., Rigoni, F. and Giacometti, G.M. (1990) *Photochem. Photobiol.* 52, 1187–1206.
- [5] Hemelrijk, P.W., Kwa, S.L.S., Van Grondelle, R. and Dekker, J.P. (1992) *Biochim. Biophys. Acta* 1098, 159–166.
- [6] Jansson, S. (1994) *Biochim. Biophys. Acta* 1184, 1–19.
- [7] Kühlbrandt, W., Wang, D.N. and Fujiyoshi, Y. (1994) *Nature* 367, 614–621.
- [8] Zuber, H., Brunisholz, R. and Sidler, W. (1987) in *Photosynthesis* (Amesz J., ed.), pp. 233–271, Elsevier, Amsterdam.
- [9] Renger, G. (1992) in *The Photosystem: Structure, Function and Molecular Biology* (Barber, J., ed), pp. 45–99, Elsevier, Amsterdam.
- [10] Holzwarth, A.R. (1989) *Q. Rev. Biophys.* 22, 239–326.
- [11] Reddy, N.R.S., Lyle, P.A. and Small, G.J. (1992) *Photosynthesis Res.* 31, 167–194.
- [12] Sundström, V. and Van Grondelle, R. (1991) in *Chlorophylls* (Scheer, H.), pp. 1125–1151, CRC Press, Boca Raton, FL.
- [13] Kenkre, V.M. and Knox, R.S. (1976) *J. Lumin.* 12, 187–193.
- [14] Nedbal, L. and Szöcs, V. (1986) *J. Theor. Biol.* 120, 411–418.
- [15] Pearlstein, R.M. (1992) *Photosynth. Res.* 31, 213–226.
- [16] Bittner, T., Wiederrecht, G.P., Irrgang, K.-D., Renger, G. and Wasielewski, M.R. (1995) *Chem. Phys.*, in press.
- [17] Voigt, J., Bittner, T. and Kehrberg, G. (1991) *Phys. Stat. Sol.(b)* 166, 135–144.
- [18] Berthold, D.A., Babcock, G.T. and Yocum, C.F. (1981) *FEBS Lett.* 134, 231–234.
- [19] Irrgang, K.D., Boekema, E.J., Vater, J. and Renger, G. (1988) *Eur. J. Biochem.* 178, 209–217.
- [20] Ruban, A.V. and Horton, P. (1992) *Biochim. Biophys. Acta* 1102, 30–38.
- [21] Huff, L. and DeShazer, L.G. (1970) *J. Optical Soc. Am.* 60, 157–165.
- [22] Bittner, T., Voigt, J., Kehrberg, G., Eckert, H.-J. and Renger, G. (1991) *Photosyn. Res.* 28, 131–139.
- [23] Kehrberg, G., Voigt, J. and Bittner, Th. (1990) *Studia Biophys.* 137, 195–206.
- [24] Leupold, D., Stiel, H., Klose, E. and Hoffmann, P. (1989) *Ber. Bunsenges Phys. Chem.* 93, 371–374.
- [25] Breton, J., Geacintov, N.E. and Swenberg, D.E. (1979) *Biochim. Biophys. Acta* 548, 616.
- [26] Ide, P.J., Klug, D.R., Kühlbrandt, W., Giorgi, L.B. and Porter, G. (1987) *Biochim. Biophys. Acta* 893, 349–364.
- [27] Bittner, T., Irrgang, K.D., Renger, G. and Wasielewski, M. (1994) *J. Phys. Chem.* 98, 11821–11826.
- [28] Kwa, S.L.S., Groeneveld, F.G., Dekker, J.P., Van Grondelle, R., Van Amerongen, H., Lin, S. and Struve, W.S. (1992) *Biochim. Biophys. Acta* 1101, 143–146.
- [29] Lin, S., Van Amerongen, H. and Struve, W.S. (1991) *Biochim. Biophys. Acta* 1060, 13–24.
- [30] Shepanski, J.F. and Anderson, R.W. (1981) *Chem. Phys. Lett.* 78, 165–173.
- [31] Bittner, T., Voigt, J., Irrgang, K.-D. and Renger, G. (1993) *Photochem. Photobiol.* 57, 158–162.
- [32] Jennings, R.C., Zucchelli, G. and Garlaschi, F.M. (1990) *Biochim. Biophys. Acta* 1016, 259–265.
- [33] Eckert, H.-J., Renger, G., Bernarding, J., Faust, P., Eichler, H.J. and Salk, J. (1987) *Biochim. Biophys. Acta* 893, 208–218.